Volume 1 | Number 1 | Jan 2013 | Pages 1–100

Polymer Chemistry

www.rsc.org/polymers

ROYAL SOCIETY OF CHEMISTRY

This is an *Accepted Manuscript*, which has been through the Royal Society of Chemistry peer review process and has been accepted for publication.

Accepted Manuscripts are published online shortly after acceptance, before technical editing, formatting and proof reading. Using this free service, authors can make their results available to the community, in citable form, before we publish the edited article. We will replace this *Accepted Manuscript* with the edited and formatted *Advance Article* as soon as it is available.

You can find more information about *Accepted Manuscripts* in the **Information for Authors**.

Please note that technical editing may introduce minor changes to the text and/or graphics, which may alter content. The journal's standard **Terms & Conditions** and the **Ethical guidelines** still apply. In no event shall the Royal Society of Chemistry be held responsible for any errors or omissions in this *Accepted Manuscript* or any consequences arising from the use of any information it contains.

Journal Name

ARTICLE

Microstructure and Melt Properties of CO-Ethylene Copolymers with Remarkably Low CO-Content

Saeeda S. Soomro,[a] Daniela Cozzula,[a] Walter Leitner,[b] Henning Vogt [a] and Thomas E. Müller [a]*

Polyketones with low CO content and molecular weight in the oligomer range were obtained with non-precedent efficiency by a new protocol for the palladium-catalysed copolymerisation of CO and ethylene. Key physicochemical properties, such as resistance to degradation and melting point were traced back to the microstructure of the polyketones. With properties tailored to the application, non-alternating polyketones emerge as interesting materials for demanding applications, where alternating polyketones are currently being used. Furthermore, the keto groups constitute interesting anchoring sites for introducing functionality.

Introduction

The copolymerisation of highly polar with non-polar monomers remains a major challenge in catalysis due to the diverging reactivity of the monomers. The factors governing the physicochemical properties of the resulting copolymers are only poorly understood as domains with deviating inter-molecular interactions are present in the material in vicinity. Thus, materials [1] made from alternating copolymers of carbon monoxide (polar) with ethylene (non-polar) [2-7] are normally highly brittle due to their crystallinity and melt only at quite high temperatures (~260°C) making processing difficult.[8, 9]

To reduce the inter-chain dipolar interactions, it was proposed to lower the concentration of CO groups along the polymer chains.[10] The use of a palladium-phosphinesulfonato complex [11] as catalyst enables successive insertion of several ethylene units, and hence synthesis of polyketones with non-alternating sequence of the monomers. However, synthesis of polyketones with low CO content [10, 12-15] was associated with strongly reduced catalyst activity compared to the strictly alternating CO-ethylene copolymerization. The lack of an adequate synthesis protocol impeded so far detailed studies concerning structure-property relationships of non-alternating polyketones. After having developed an improved highly efficient protocol for the non-alternating copolymerization of CO and ethylene, we were able to obtain a series of non-alternating polyketones varying in CO content. The current study is targeted at elucidating the physicochemical properties of such polymers in dependence of their microstructure.

Results and discussion

Copolymers of CO and ethylene were obtained using a palladium catalyst prepared *in-situ* from Pd(OAc)$_2$ and 2-(*bis*-(2-methoxyphenyl)phosphino)benzenesulphonic acid (**HL**, Scheme 1). Three factors proved to be crucial to achieve outstanding catalyst activities: (*i*) To avoid catalyst decomposition during the initial phase of the reaction, the reaction was started by injecting a solution of Pd(OAc)$_2$/**HL** in CH$_2$Cl$_2$ into a solution saturated with a mixture of CO and ethylene at reaction temperature. (*ii*) During the reaction, the pressure in the reactor was maintained constant at 50 bar, replacing consumed CO and ethylene by feeding a CO-C$_2$H$_4$ gas mixture (semi-batch operation). Note that due to preferential incorporation of CO into the polymer the gas phase became gradually depleted of CO with time. (*iii*) The CO content in the gas phase was kept low by controlling the composition of the gas-mixture flowing into the reactor.
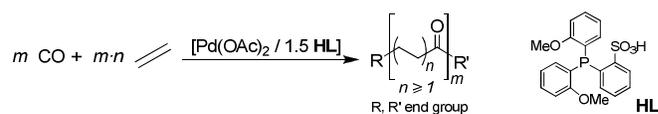
Scheme 1. Synthesis of polyketones by palladium-catalysed copolymerization of CO and ethylene (on average, n > 1 for non-alternating polyketones).

Polyketones **P1**, **P2**, **P3** and **P4** with decreasing CO content were obtained by lowering the CO/C$_2$H$_4$ ratio in the gas mixture stepwise from 15/35 to 12/38, 6/44 and 1/49, respectively.[†] Analysis of the bulk composition of the resulting polymers by high-temperature ^{1}H NMR spectroscopy (*vide infra*) showed that the CO content was 28.9, 16.1, 3.7 and 2.5 wt% of the polymer, respectively (Table 1). Prolonging the reaction time with consequentially higher consumption of CO-C$_2$H$_4$ gas mixture (10.7 → 33.2 g) provided a polymer with lower CO content (**P4** → **P5**, 2.5 → 1.5 wt%, respectively). When the catalyst loading was reduced (0.05 → 0.01 mmol), while retaining a short reaction time, the CO content increased from

2.5 *via* 2.4, 5.5 to 13.5 wt% (**P4**, **P6**, **P7**, **P8**, respectively). By contrast, varying the reaction temperature in the range 100 – 130°C (10°C increments, **P9**, **P4**, **P10** and **P11**, respectively) had little influence on the CO content (2.4 – 3.0 wt%). Altogether, the parameter study shows that the CO content in the polymers is readily adjusted in a wide range, whereby the CO/C_2H_4 ratio in the feed has the most pronounced impact.

Table 1. Conditions for the synthesis of polyketones **P1** to **P11** and selected chemical and structural data.[a]

Poly-ketone	c(Pd)[b] [10^{-3} mol·l^{-1}]	Ratio CO/C_2H_4	T [°C]	CO content [wt%]	$\nu_{C=O}$[c] [cm^{-1}]	No. of branches[d] [%]	M_n[e] [g·mol]
P1	0.05	15/35	110	28.9	1694	1.54	-
P2	0.05	12/38	110	16.1	1707	0.24	3077
P3	0.05	6/44	110	3.7	1712	0.59	2843
P4	0.05	1/49	110	2.5	1713	0.20	5272
P5	0.05	1/49	110	1.5	1716	0.17	3919
P6	0.037	1/49	110	2.4	1710	0.28	5413
P7	0.025	1/49	110	5.5	1709	0.27	5827
P8	0.01	1/49	110	13.5	1707[f]	0.06	5408
P9	0.05	1/49	100	2.4	1712	0.18	5610
P10	0.05	1/49	120	3.0	1711	0.25	3580
P11	0.05	1/49	130	2.4	1714	0.41	2539

[a] For synthesis of reference samples **R1** and **R2** refer to supplementary information (SI);[†] [b] Ratio Pd(OAc)$_2$/HL 1/1.5, CH_2Cl_2, 50 bar; [c] Maximum of the $\nu_{C=O}$ vibration; [d] Average number of methyl groups per ethylene unit determined by ^{1}H NMR spectroscopy; [e] Determined by GPC chromatography; [f] Three distinct maxima at 1713, 1702 and 1693 cm^{-1}.

Analysis of the polyketones by IR spectroscopy showed a maximum of the characteristic band for the CO stretch vibration in the range 1694-1716 cm^{-1} (Table 1), whereby the wave number at which the maximum occurred decreased (at increasing intensity) with increasing CO content.[†] Closer inspection of the CO signal revealed three distinct contributions (Figure 1). Comparison of the signal shape in the spectrum of **P2** (CO content 16.1 wt%) with the spectra of reference sample **R2** with very low CO content (0.7 wt%) and polyketone **R1**
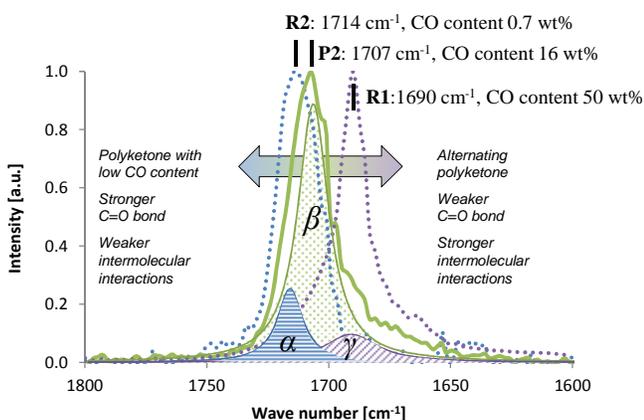
Figure 1. Comparison of the carbonyl region of the IR spectra of polyketone **P2** (middle) with that of reference material **R2** with very low CO content (left) and polyketone **R1** with alternating CO and C_2H_4 units (right). The spectrum of **P2** was

deconvoluted and the contribution of moieties α, β and γ is shown. For better visualization, the signal intensity was normalized.

obtained by strictly alternating CO-C_2H_4 copolymerisation with Pd(OAc)$_2$/DPPPr (DPPPr = *bis*-diphenylphosphinepropane) [16] allowed the assignment of these three contributions to: (α) isolated CO moieties separated by oligomeric –$(C_2H_4)_n$– segments, (β) non-alternating segments with CO moieties in the vicinity, and (γ) segments with alternating CO and C_2H_4 units (Scheme 2). Furthermore, sets of bands characteristic for methylene groups were observed at 2914, 2847 (ν_{CH} stretch), 1472, 1462 (ν_{CH} bend) and 729, 718 cm^{-1}, respectively (ν_{CH} rock).[17-19] The position of these signals closely resembled those of a polyethylene reference sample **PE** obtained by homo-polymerization of ethylene, thereby suggesting the presence of polyethylene-like segments in the polyketones.[†]
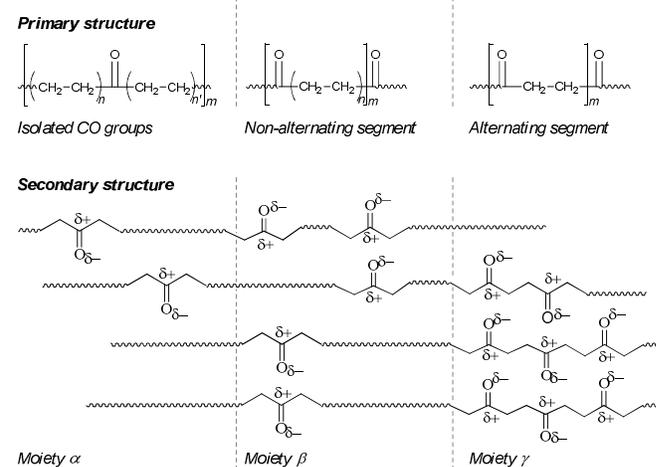
Scheme 2. Structural moieties α, β and γ present in the primary structure of non-alternating polyketones give rise to a secondary structure with regions characterised by different strength of intermolecular interactions.

Taking this information into account, the IR signals of the entire series of non-alternating polyketones obtained in this study were deconvoluted.[20] The extinction coefficient of the CO stretch vibration of moieties α-γ was assumed to be equal as moieties α-γ represent chemically similar environments. For all polyketones, the carbonyl vibration was adequately described by a single Lorentzian function for each of the three contributions α, β and γ centred at 1716, 1706 and 1691 cm^{-1}, respectively. This suggests that analogous moieties were present in the series of materials. The assignment is supported by comparison with alternating polyketones containing propene as co-monomer, for which a Raman band at ≥1709 cm^{-1} increasing in intensity with increasing propene content was assigned to CO moieties in a disordered local environment similar to moieties β.[22]

With increasing CO content, the relative contribution of moiety α decreased sharply (Figure 2). The contribution of moiety β increased steadily up to a CO content of 16 wt% and then decreased at higher CO content. The contribution of moiety γ showed sinusoidal characteristics with a sharp increase related

to the decrease in the contribution of moiety β. The three different structural entities are characterized by a distinct local environment of the CO groups in the secondary structure of such non-alternating polyketones. The shift to lower wave numbers in the series $\alpha \rightarrow \beta \rightarrow \gamma$ (Figure 1) is consistent with reduced bond order in a polar local environment.[21] Isolated CO moieties (α) are surrounded mostly by non-polar methylene groups. CO moieties in non-alternating segments (β) are involved in dipolar interactions, whereas CO moieties in fully alternating segments (γ) are stacked into a semi-crystalline environment with strong intermolecular interactions (*vide infra*).
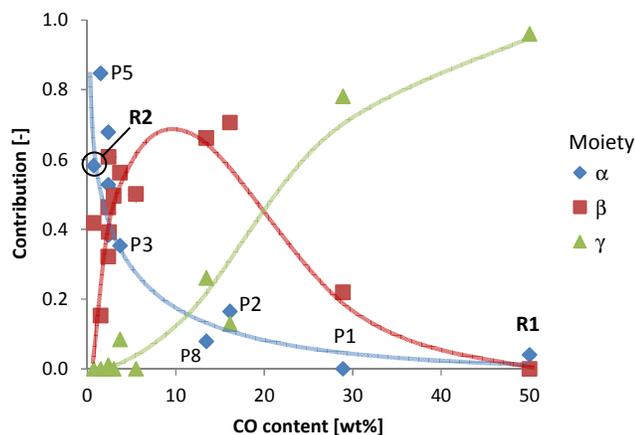
Figure 2. Contribution of moieties α, β and γ to the intensity of the CO stretch vibration in the IR spectra of polyketones **P1**-**P11** and reference samples **R1**, **R2**.

To unravel the microstructure, samples were characterised by NMR spectroscopy, which was performed at 95°C to enhance the solubility of the polymer (C_6D_5Cl, Figure 3). In the ^{1}H NMR spectrum of **P4** (discussed here as the most representative sample of this series of polyketones) characteristic signals at 2.38 and 1.67 ppm were assigned to the methylene groups in alpha and beta position to the carbonyl group (non-alternating segments, **G** and **F**, respectively). Methylene groups in alternating segments (**J**, corresponding to moieties γ) gave rise to a signal at 2.64 ppm and the oligomeric –(C_2H_4)$_n$– segments (**E**) to an intense signal centred at 1.46 ppm. More detailed analysis of the spectrum revealed characteristic signals for terminal olefinic groups (–CH=, **B** and =CH$_2$, **A** at 5.91 and 5.08 ppm, respectively; relative intensity 1:2) as well as methyl groups (**L** at 1.02 ppm). These signals can be assigned to end groups of the polymer chains indicating that the growth of individual polymer chains was terminated by chain transfer through β-hydride elimination. This suggests that the Pd-H group [23] formed in the chain transfer step is able to initiate the growth of a subsequent polymer chain (*vide infra*), giving rise to polymer chains terminated by a vinyl group on the one side and a methyl group on the other side. Closer inspection of the ^{1}H NMR spectra showed that some of the double bonds migrated along the polymer chains, resulting in a signal characteristic for internal double bonds (–CH=CH–, **D** at 5.54 ppm). Noteworthy, the corresponding methyl groups had a

higher intensity than anticipated from the intensity of the alkene groups; this indicates that repeated ß-hydride elimination and re-insertion of the resulting alkene led to formation of additional methyl branches along the polymer chains. An alternative mechanism of formation of methyl groups *via* bimolecular hydride transfer to an incoming ethylene molecule, therefore, appears unlikely.
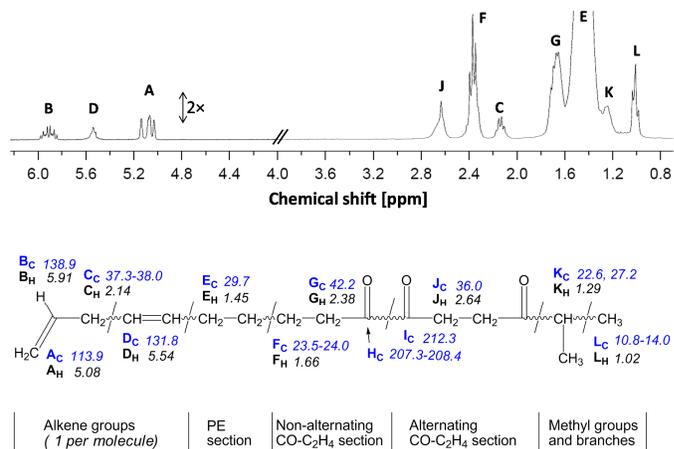
Figure 3. Selected range of the ^{1}H NMR spectrum of **P4** and assignment of the chemical moieties in the ^{1}H and ^{13}C NMR spectra (chemical shift in ppm).

The microstructure of the polyketones was confirmed by analysis of the $^{13}C\{^1H\}$ NMR spectra.[24] Noteworthy, the position of the different signals was similar for the entire series of polyketones, indicating that the carbon spectrum is dominated by the architecture of the polymer chain. The CO group of non-alternating segments (**H,** moieties $\alpha+\beta$) gave rise to characteristic signals in the range of 207.3-208.4 ppm. This compares with 212.3 ppm for the keto group of the alternating segments (**I**) in reference sample **R1**. Polyketone **P9** showed a further signal at 202.8 ppm tentatively attributed to a CO group nearby an internal double bond. The characteristic signals for the methylene groups in alpha and beta position to the carbonyl group in non-alternating segments were observed at 42.1-42.6 ppm (**F**) and 23.5-24.0 ppm (**G**), respectively. Methylene groups in alternating segments (**J**, moieties γ) gave rise to a signal at 36.0 ppm, which compares with 35.6-35.8 ppm for reference sample **R1**. A further feature is a signal at 37.3-38.0 ppm, which is tentatively assigned to short alternating segments (**J**). The oligomeric –(C_2H_4)$_n$– segments (**E**) resulted in several signals at 28.9-30.1 ppm, which compares favourably with the polyethylene reference sample **PE** (29.7 ppm). More detailed analysis of the spectra confirmed the presence of signals characteristic for terminal olefinic groups (–CH=, **B** and =CH$_2$, **A** at 138.9 and 113.9-114.0 ppm, respectively) and internal double bonds (–CH=CH–, **D** at 131.8 ppm). Interestingly, the methyl (**K**) as well as the methine groups (**L**) gave rise to several signals (22.6, 19.7, 13.8-14.0 ppm and 33.7, 31.9, 27.2 ppm, respectively),[24] thereby indicating that branches occurred at different positions along the polymer chain. For **P3,** a signal observed at 10.8 ppm is assigned to the methyl group of an

ethyl branch (**L**). In the spectrum of **R1**, the signal of the -CH-group occurred at a very different position (51.7 ppm assigned to -CO-C$\underline{H}$(CH$_3$)-CO-). No signal for such groups was observed for the other polyketones.

Based on a β-hydride elimination mechanism, the molecular weights of the polyketones **P2-P11** were calculated from the integrals of the ^{1}H NMR spectra to $2.5 – 5.8 \times 10^3$ g/mol (Table 1). For comparison, a living polymerization without chain transfer would give rise to a molecular weight of $132–660 \times 10^3$ g/mol. Gel permeation chromatography confirmed the molecular weight to be in the oligomer range and revealed a surprisingly narrow molecular weight distribution (PDI 1.7 – 2.3).† While the catalyst loading had no distinct influence on the molecular weight ($5.3 – 5.8 \times 10^3$ g/mol for **P8**, **P7**, **P6** and **P4**), the molecular weight notably decreased with increasing temperature (from 5.6×10^3 g/mol at 100°C (**P9**) → 2.5×10^3 g/mol at 130°C (**P11**)). This strong dependency clearly shows that the chain transfer mechanism becomes more prominent with increasing temperature consistent with higher activation energy of the chain transfer step compared to the chain elongation reaction. Similarly, the number of methyl groups along the polymer chain increased with the reaction temperature (100 → 130°C, increase from 0.18, 0.20, 0.25 to 0.41 % of the incorporated ethylene units, **P9**, **P4**, **P10** and **P11**, respectively). Thus, also the propensity towards repeated ß-hydride elimination and re-insertion of the growing chain becomes more prominent at higher temperatures.
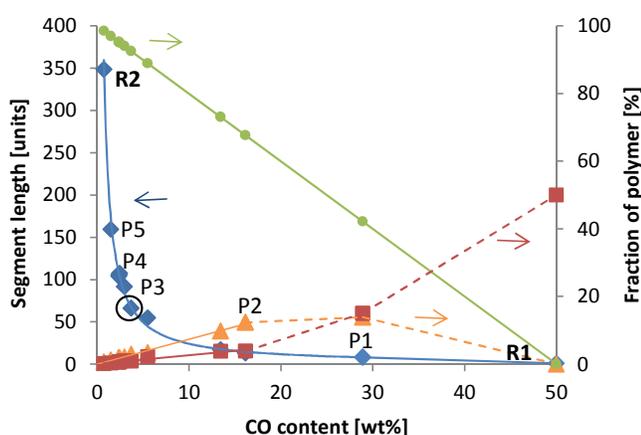
Figure 4. Relation of the average segment length in moieties α (♦), CH$_2$ groups in non-alternating (▲) and alternating CO-C$_2$H$_4$ segments (■) and the CO content in polyketones **P1-P11** in comparison to reference samples **R1** and **R2**. For comparison, the fraction of oligomeric –(C$_2$H$_4$)$_n$– segments (PE, ●) is also shown.

With increasing CO content in the polyketone, the average length of the oligomeric –(C$_2$H$_4$)$_n$– segments in moieties α decreased sharply, following the empirical correlation *segment length = 2,63 × (CO content/100%)$^{-1}$* (Figure 4). Accordingly, the average length of the segments decreased from 159 units at a CO content of 1.5 wt% (**P5**) to 66 units at a CO content of 3.7 wt% (**P3**). This compares with a segment length of 348 units at a CO content of 0.7 wt% (**R2**) and 1 unit for a fully alternating polyketone (**R1**). In parallel, the content

of oligomeric –(C$_2$H$_4$)$_n$– segments, which are not influenced by the presence of neighbouring CO groups in the polymer chain, decreased from 97.0 wt% (**P5**) to 42.2 wt% (**P1**). Interestingly, the content of CH$_2$ groups neighbouring isolated and non-alternating CO-C$_2$H$_4$ segments (moieties α and β), increased linearly with the CO content from 1.2 wt% (**P5**) to a maximum at 14 wt% (**P1**) and then decreased to zero for the alternating polyketone **R1**.†

As it was expected that the changing strength of the inter-molecular forces substantially affects the macroscopic properties, selected physicochemical parameters (melting point, viscosity of the melt, decomposition temperature) were investigated for the series of non-alternating polyketones (Table 2).

Table 2. Physicochemical properties of polyketones **P1** to **P11** in comparison to reference samples **R1**, **R2** and **PE**.

Poly-ketone	CO content [wt%]	T_m (T_g) ^{a} [°C]	ΔH_m* (ΔH*) ^{a} [J/g]	Melt viscosity ^{b} [Pa·s]	T_d ^{d} [°C]	Weight loss [%]
R1	50.0	(72)	(2.5)	- ^{c}	339	58.0
P1	28.9	(122/132)	(3.1/3.3)	- ^{c}	245/395	13.2/53.9
P2	16.1	(120)	(77)	- ^{c}	233/431	8.1/74.8
P3	3.7	(127)	(130)	- ^{c}	223/451	3.5/83.3
P4	2.5	125	218	1.29	469	96.2
P5	1.5	125	219	0.80	464	97.5
P6	2.4	125	218	0.93	468	95.9
P7	5.5	126	202	1.12	467	94.5
P8	13.5	119-124	141	1.47	216/452	3.1/87.5
P9	2.4	128	216	3.20	465	97.0
P10	3.0	124	200	0.51	469	96.0
P11	2.4	121	200	0.16	467	96.1
R2	0.7	127	169	- ^{c}	464	98.0
PE	0	126	211	0.52	468	99.6

^{a} Phase transitions were followed by differential scanning calorimetry; T_g, ΔH* for **P1-P3** and **R1**; T_m, ΔH_m* for **P4-P11**, **R2** and **PE**; ^{b} at 160°C; ^{c} Sample does not melt at ≤ 220°C; ^{d} Onset temperature of weight loss.

Interestingly, polyketones **P4**-**P11** were characterized by a low melting point in the range of 121-128°C similar to the melting point of reference samples **R2** and **PE** with very low or no CO content. Melting of the polyketones was associated with a high specific heat ΔH_m* (202-219 J·g^{-1}), except **P8**, which displayed a lower heat of melting (141 J·g^{-1}). By contrast, polyketones **P1**-**P3** with high CO content did not melt below 220°C, which is consistent with the high melting point of 257°C reported for alternating polyketones.[16] Polyketones **P1**-**P3** instead showed an endothermic signal in differential scanning calorimetry (Table 2), which was observed at a similar temperature for **P3** (127°C), **P2** (120°C) and **P1** (double signal at 122, 132°C) as melting for the other polyketones. In contrast, this signal was observed at a considerably lower temperature for **R1** (72°C). The intensity of the endothermic signal decreased in the same sequence (130, 77 and 6.4 J·g^{-1} for **P3**, **P2** and **P1**, respectively, compared to 2.5 J·g^{-1} for **R1**). These features suggest that this transition is associated with glass transition.[25] A change of the crystalline fraction from the alpha modification to the beta form

(analogous to alternating polyketones,[26] *vide infra*) appears less likely as polyketones **P4**-**P11** show a distinct melting point at a similar temperature.

Closer inspection of the physicochemical properties revealed that the phase behaviour was related to the content of α, β and γ moieties. The low-melting polyketones **P4**-**P11** (except **P8**, *vide infra*) were characterized by the absence of γ moieties.[†] In contrast, polyketones **P1**-**P3** showing a low temperature glass transition are characterized by a certain content of γ moieties. Parallel to increasing γ content (0.08→0.13→0.78 for **P3**, **P2** and **P1**, respectively), the temperature and the enthalpy of the glass transition decreased. Similarly, reference sample **R1** with very high γ content had a very low enthalpy of the low-temperature glass transition (2.5 J/g). For polyketone **P8**, the much lower enthalpy of melting compared to that of the other polyketones in the series **P4**-**P11** also seems to be related to the considerable content of γ moieties (0.26). It is surmised that in **P8**, the alternating polyketone segments were not evenly distributed along the polymer chains giving rise to the somewhat different properties. Further, a linear dependency was evident between the enthalpy of melting and the length of the oligomeric $-(C_2H_4)_n-$ segments in the series **P6**, **P7** and **P8** with similar molecular weight (Figure 5). This suggests that the melt transition is dominated by the polyethylene character in these polymers rather than by the interactions between the CO units.
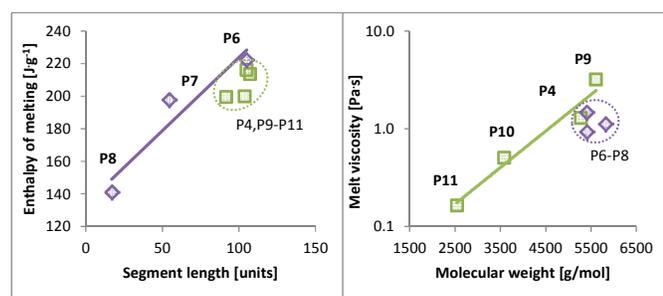
Figure 5. Change of the enthalpy of melting (left) and melt viscosity (right) in the series of polyketones **P6**-**P7**-**P8** varying in CO-content (diamonds) and **P9**-**P4**-**P10**-**P11** varying in molecular weight (squares).

The melt viscosities of polyketones **P4**–**P11** recorded at 160°C showed a visible decrease in the viscosity with increasing shear rate (< 200 s^{-1}). This shear thinning effect was most pronounced for **P8**, whereas it was hardly observed for **P11**. Such shear thinning frequently occurs in samples with elongated polymer coils (*vide infra*).[27] At higher shear rates (200-770 s^{-1}), the melt viscosity of polyketones **P4**–**P11** was in the range of 0.16 – 3.20 Pa·s. Noteworthy, for polyketones **P9**, **P4**, **P10** and **P11** with similar CO content, the melt viscosity showed an exponential decrease with decreasing molecular weight (Figure 5). Such higher order dependence of viscosity and molecular weight is also typical for ellipsoidal polymer coils.[27] By contrast, in the sequence of **P6**, **P7** and **P8** differing in CO content but displaying similar molecular weight, only a slight increase in viscosity with increasing CO content was observed

(0.92, 1.11 and 1.46 Pa·s, respectively). Thus, the melt viscosity is governed mostly by the molecular weight of the polyketones. Polyketones without alternating segments (**P4**-**P7**, **P9**-**P11**) showed remarkable thermal stability. Upon heating in a stream of inert gas, the onset temperature of a weight loss (T_d) was observed as high as 464-469°C; decomposition was associated with a weight loss of 93-98%. This high thermal stability resembles the performance of polyethylene (**PE**: T_d 468°C, 99.6% weight loss). In contrast, polyketones with alternating segments (**P1**-**P3**, **P8**) showed two steps of thermal degradation at 216-245°C and 395-452°C that were associated with a weight loss of 3-13% and 54-88%, respectively. The weight loss was related directly to the CO content; samples with higher CO content showed a higher weight loss in the first step and a lower weight loss in the second step. This is in contrast to alternating polyketone **R1**, for which a single step was observed (T_d 339°C, 58.0% weight loss) and indicative of two distinct degradation mechanisms.

Changes in the strength and direction of the intermolecular interactions also affect the crystallinity of the materials. Thus, the powder XRD diffractogram of **R1** was marked by the characteristic reflections for the α-form of alternating polyketone at 2Θ 21.71° [110 reflection, *vs*] and 25.90° [200, *s*] as well as by a series of weaker reflections at 24.75° [111], 31.41° [210] and 41.91° [301].[28, 29] A reflection at 29.46° with low intensity indicates the presence of a small amount of the ß-form [210]. With the CO content decreasing in the series **P1**, **P2**, **P3**, **P4**, the position of the very strong signal at 21.71° shifted slightly to lower 2Θ values (21.49°), while the other reflections decreased in intensity, instead giving rise to a new strong reflection at 23.88° and a series of weaker reflections.[†] The same set of signals as for **P4** was also observed for all other samples (**P5** to **R2**). Comparison with the powder diffractogram of **PE** showed that these reflections are characteristic for domains of polycrystalline polyethylene.

The content of the crystalline fraction was calculated from the difference between the heat taken up during melting and the heat released during solidification.[†] Among polyketones **P9**, **P4**, **P10** and **P11** with similar CO content, the crystalline fraction (18.1, 17.2, 17.0 and 12 %, respectively) decreased linearly with the concentration of methyl branches along the polymer chain (0.18, 0.20, 0.25 and 0.41 %, respectively). Thus, such short branches disturb the alignment of neighbouring polymer chains. This trend is analogous to alternating polyketones where propene was incorporated as co-monomer to reduce the crystallinity of the material.[22] For samples **P6**, **P7** and **P8** characterized by varying CO content, the content of the crystalline fraction (46.9, 21.5 and 16.7 %, respectively) decreased steadily with decreasing length of the oligomeric $-(C_2H_4)_n-$ segments (105.1, 54.6 and 17.1 units, respectively). Thus, it appears also here that the polyethylene character dominates over the polyketone character.

Experimental

Materials

Chemicals were obtained from commercial suppliers and used as received, if not stated otherwise.[†] All chemical manipulations, except for polymer workup and analysis, were performed under an argon atmosphere using Schlenk techniques.

Synthesis of polyketones

Polyketones **P1** to **P11** were prepared by the copolymerization of carbon monoxide and ethylene in a 300 mL Parr high pressure reactor equipped with mechanical stirrer and cooling system. In a typical experiment (for details on the other experiments, see Table 1 and SI [†]), a glass liner was charged with freshly distilled dichloromethane (100 mL) and placed into the reactor. After closing, the reactor was purged with argon and then pressurized with a mixture of CO and ethylene to 10-15 bar. The reactor was then heated to 110 °C. In parallel, a 30 ml gas burette was charged with a solution of $Pd(OAc)_2$ (11.22 mg, 0.05 mmol) and **HL** (30.18 mg, 0.075 mmol) in dichloromethane (5 mL) and connected to the reactor. The gas burette was pressurized with the same mixture of CO and ethylene to 60 bar and the solution introduced into the reactor. Immediately thereafter, the pressure was adjusted with the CO-ethylene mixture to 50 bar. Afterwards, the pressure was kept stable by feeding the CO-ethylene mixture using a mass flow controller (Bronkhorst), whereby the consumption of the gas mixture was recorded. At the end of the reaction, the gas supply was discontinued, and the reactor was cooled down to room temperature and vented. The polymer was collected by vacuum filtration as white powder, washed three times with dichloromethane (50 ml) and dried for at least five hours at 60 °C in a partial vacuum.

The reference sample **R1** was prepared by CO-C_2H_4 copolymerization with a catalyst generated *in situ* from an equimolar amount of $Pd(OAc)_2$ and diphenylphosphinopropane (DPPPr).[16] The reference sample **R2** was prepared following a method adapted from literature [12] using a higher catalyst loading ($Pd(OAc)_2$, 44.9 mg, 0.2 mmol; **HL**, 120.7 mg, 0.3 mmol in dichloromethane, 25 mL). The reference sample **PE** was obtained in the same way, except that the reaction was carried out with ethylene as the only reactive gas and that [Pd(**HL**)(1-η^2,5η^1-6-ethoxy-exo-5,6-dihydrodicyclopenta-diene)] was used as catalyst.

Characterization of polyketones

FT-IR spectra were recorded on an ALPHA FT-IR Spectrometer (Bruker Optics) equipped with a diamond probe. A sample of the polymer (**R1, P1**-**P11, R2**) was scanned 32 times with a resolution of 8 cm^{-1}. The data was collected in the range of 4000–400 cm^{-1} and analysed using OPUS 7.0 (Bruker Optics) as software. For deconvolution of the CO stretch vibration, spectra were collected in the range of 1800-1600 cm^{-1} with a resolution of 2 cm^{-1}. The CO signal was deconvoluted

using a combination of three Lorentzian functions $L(\nu) = (I/\pi) \times 0.5 \times (\Gamma \times (\nu - \nu^0)^2 + (0.5 \times \Gamma)^2)^{-1}$, whereby I is the parameter describing the intensity, ν^0 the position and Γ the width of the contribution of a particular moiety to the IR signal of the CO stretch vibration. Fitting parameters were the intensity of the individual contributions I_i and, in case of polymers **R1** and **P8**, the width Γ_i. The position ν_i and the width Γ_i (except **R1** and **P8**) of the contributions of moieties α, β and γ were refined to a common position. Details on further characterisation of the polyketones are given in the SI.[†]

Conclusions

A series of CO-ethylene copolymers varying in CO content was synthesised, whereby outstanding catalyst activities were obtained by adopting an innovative reaction engineering approach. Analysing the trends throughout the series, it was demonstrated that the physicochemical properties can be traced back to the microstructure of the polyketones. Three different chemical moieties α, β and γ were identified, which are characterised by the specific local density of CO groups along the polymer chain. Segments with high CO density give rise to domains with strong intermolecular dipole-dipole interactions (moieties γ), which dominate the phase change behaviour, while the melt viscosity decreases rapidly with decreasing molecular weight. Significant shear thinning of the polymer melt under physical strain is thereby indicative of the formation of elongated polymer coils. The crystallinity of the CO-ethylene copolymers is related directly to the length of the oligomeric –$(C_2H_4)_n$– segments suggesting that the polyethylene character dominates over the polyketone character. Also the presence of methyl branches along the chain has a strong influence of the material properties in the solid state leading to reduced crystallinity and, in consequence, reduced enthalpy of melting. Processing is facilitated by the outstanding thermal stability of the copolymers, which ensures a sufficiently wide processing window.

In summary, the physicochemical properties of CO-ethylene copolymers are governed by the primary structure (CO content, molecular weight and the concentration of methyl branches along the chain) and the secondary structure consequentially formed (moieties α, β and γ). In turn, the primary structure can be regulated by choosing the conditions during the synthesis of the CO-ethylene copolymers. Such detailed understanding of how structural features translate into macroscopic properties is the key to tailoring the properties of CO-ethylene copolymers to the requirements of specific applications. Additionally, the keto groups provide an option to introduce other functional groups allowing, *e.g*., for cross-linking and curing of the material after processing or for introducing specific functions into the materials.

Acknowledgements

Notes and references

[a] CAT Catalytic Center, RWTH Aachen University, Worringerweg 1, 52074 Aachen, Germany. Fax: 49 241 80 28594; Tel: 49 241 80 22593; E-mail: thomas.mueller@catalyticcenter.rwth-aachen.de.

[b] Lehrstuhl für Technische Chemie und Petrolchemie, Institut für Technische und Makromolekulare Chemie, RWTH Aachen University, 52074 Aachen, Germany.

1. R. Farris and J. W. Kelly, *Plastics Technology (USA)*, 1997, **43**, 50-53.
2. C. E. Ash, *Int. J. Polym. Mat.*, 1995, **30**, 1-13.
3. C. Cheng, D. Guironnet, J. Barborak and M. Brookhart, *J. Am. Chem. Soc.*, 2011, **133**, 9658-9661.
4. A. A. Broekhuis, Y. Zahng, F. Picchioni and A. J. M. Roks, *Eur. Pat. Appl.*, 2010, EP2174973A2174971.
5. H. J. Guinn and R. L. Mahlon, *Eur. Pat. Appl.*, 2000, EP1045017.
6. V. J. Notogiacomo, *US Pat. Appl.*, 1991, US5030674.
7. E. Drent, J. A. M. v. Broekhoven and M. J. Doyle, *J. Organomet. Chem.*, 1991, **417**, 235-251.
8. F. Garbassi, A. Sommazzi, L. Meda, G. Mestroni and A. Sciutto, *Polym.*, 1998, **39**, 1503-1506.
9. G. A. Holt and J. E. Spruiell, *J. Polym.*, 2002, **83**, 2124-2142.
10. R. Luo, D. K. Newsham and A. Sen, *Organometallics*, 2009, **28**, 6994-7000.
11. A. Nakamura, T. M. J. Anselment, J. Claverie, B. Goodall, R. F. Jordan, S. Mecking, B. Rieger, A. Sen, P. W. N. M. van Leeuwen and K. Nozaki, *Acc. Chem. Res.*, 2013 **46**, 1438-1449.
12. E. Drent, R. v. Dijk, R. v. Ginkel, B. v. Oort and R. I. Pugh, *Chem. Commun.*, 2002, 964-965.
13. A. K. Hearley, R. J. Nowack and B. Rieger, *Organometallics*, 2005, **24**, 2755-2763.
14. L. Bettucci, C. Bianchini, C. Claver, E. J. G. Suarez, A. Ruiz, A. Meli and W. Oberhauser, *Dalton Trans.*, 2007, 5590-5602.
15. E. J. García Suárez, C. Godard, A. Ruiz and C. Claver, *Eur. J. Inorg. Chem.*, 2007, **18**, 2582-2593.
16. E. Drent, J. A. M. Vanbroekhoven and M. J. Doyle, *J. Organomet. Chem.*, 1991, **417**, 235-251.
17. R. Gooden, D. D. Davis, M. Y. Hellman, A. J. Lovinger and F. H. Winslow, *Macromolecules* 1988, **21**.
18. S. Krimm, C. Y. Liang and G. B. B. M. Sutherland, *J. Chem. Phys.*, 1956, 549-563.
19. E. Pretsch, T. Clerc, J. Seibl and W. Simon, in *Tabellen zur Strukturaufklärung organischer Verbindungen mit spektroskopischen Methoden*, Springer Heidelberg, 1990.
20. D. Engel, PEAXACT 3.0.7 - Software for Quantitative Spectroscopy and Chromatography, S•PACT GmbH, Aachen, Germany, 2013.
21. T. W. Lai and A. Sen, *Organometallics*, 1984, **3**, 866-870.
22. J. M. Lagaron, A. K. Powell and N. S. Davidson, *Macromol.*, 2000, **33**, 1030-1035.
23. J. P. Collman, L. S. Hegedus, J. R. Norton and R. G. Finke, *Principles and Applications of Organotransition Metal Chemistry*, University Science Books, 1987.
24. E. W. Hansen, R. Blom and O. Bade, *Polym.*, 1997, **38**, 4295-4304.
25. N. Hayki, N. Desilles and F. Burel, *Polym. Chem.*, 2011, **2**, 2350-2355.
26. Y. Chatani, T. Takizawa, S. Murahashi, Y. Sakata and Y. Nishimura, *J. Polym. Sci.*, 1961, **55**, 811-819.
27. T. G. Mezger, in *The Rheology Handbook, 3rd Revised Edition*, Vicent Editor, 2011.
28. E. A. Klop, B. J. Lommerts, J. Veurink, J. Aerts and R. R. Van Puijenbroek, *J. Polym. Sci. B: Polym. Phys.*, 1995, **33**, 315-326.
29. B. J. Lommerts, E. A. Klop and J. Aerts, *J. Polym. Sci. Polym. Phys. Ed.*, 1991, **31**, 1319-1330.

Polymer Chemistry Accepted Manuscript